

Exploring the Project Potential of Marine Current Turbines: A Case Study in the Southern Brazilian Shelf Region

Juliana Tavora Bertazo Pereira, Eduardo de Paula Kirinus, Wiliam Correa Marques, Tiago Borges Ribeiro Gandra, Gustavo Pessoa de Barros, Helena Barreto Matzenauer

Instituto de Oceanografia, Universidade Federal do Rio Grande, Rio Grande, Brazil
Email: tavora.pereira@gmail.com

Received 8 October 2014; revised 5 November 2014; accepted 1 December 2014

Copyright © 2014 by authors and Scientific Research Publishing Inc.
This work is licensed under the Creative Commons Attribution International License (CC BY).
<http://creativecommons.org/licenses/by/4.0/>



Open Access

Abstract

The application of marine current turbines for electricity generation could offer a distinct advantage over other renewable energy sources due to the regular and predictable nature of this resource. This paper details the application of Analytical Hierarchy Process (AHP) as a possible tool for decision makers to better understand the environment and the impacts of the marine current turbines. The best areas for generating energy from the currents were found using a tridimensional model (TELEMAC3D). In addition to applying the energy conversion module, these regions were also evaluated for energy production, which was then applied to the AHP. Several databases (Transmission and Transport, Socioeconomic, Conservation Units, Endangered Species and Geological Information) were compared to minimize decision deviation. The results showed the viability of the northern region of the Southern Brazilian Shelf (SBS) as a possible area to harvest energy from the currents, as much of the studied region was limited by human activities in the coastal zone and sensitive biological resources.

Keywords

AHP, Renewable Energies, Hydrokinetic Turbines, TELEMAC3D

1. Introduction

The continuous growth of the world population increases the demand and competition for energy, requiring an immense effort for nonrenewable energy sources availability. Therefore, in addition to promoting the development of new technologies, global policies for the generation of renewable and clean energy are being streng-

thened. Several methods of energy conversion have been developed over the years, especially the turbine-based current energy converters. These converters have demonstrated high energy generation capacity and are already in operation.

The policies for the installation of Marine Current Turbines (MCT) were compiled by examining a wide range of literature related to sustainability [1]-[3], integrated resource planning [4], and the construction of portfolios of electricity generation technologies. This research determined that few previous research studies have systematically considered the overall effects of technical, economic, social, and environmental sustainability objectives related to constructing electricity generation portfolios, according to multiple stakeholder perspectives [5].

These important parameters were considered in other studies in the USA [6]-[8], Iran [9], and Taiwan [10] [11]. These issues have not been addressed with regard to the usage of MCT in the Southern Brazilian Shelf. The recent annual energy report of the Rio Grande do Sul State [12] briefly mentioned the use of marine currents as a possible energy source for harvesting power, which could easily enhance the Brazilian matrix of energy. The main purpose of this work is to offer substantial information regarding the sustainability parameters for policy makers to improve the installation process.

In Brazil, no coastal zones have been mapped to determine the energetic potential viable for conversion using hydrokinetic turbines. Recent studies showed two areas (**Figure 1(b)** and **Figure 1(c)**) of high power availability on the coast of Rio Grande do Sul State that can generate 3.5 MW/year of power [13]. Another research project [14] studied the influence of hydrodynamic and morphodynamic processes of the installation of six hydrokinetic turbines reaching 5 GW/year annual power.

Study Area

The Southern Brazilian Shelf (SBS), located between 28°S and 35°S (**Figure 1**), is continentally bounded by the Rio Grande do Sul State. The SBS has a slightly rugged shoreline that is oriented Northeast to Southwest. The bathymetry of this region is quite soft, with the higher slope and shelf break located near the 180 m isobath [15].

The region is located near the Brazil-Malvinas Confluence zone and is known for high spatial and temporal variability and also for the convergence of several water masses [16] [17]. The Southwest Atlantic Ocean is one of the most dynamic regions of the global ocean [18] [19], characterized by large thermohaline contrasts and intense mesoscale activity [20].

The high seasonality of the wind fields [21] [22] is characterized by the dominance of northeast (NE) winds during the summer and southwest (SW) winds during the winter, which drive the coastal circulation through the SW and NE, respectively [14] [17] [23] [24]. These winds can be enhanced by El Niño Southern Oscillation (ENSO) events [21].

2. Methodology

The methodology of this work was based on the usage of a tridimensional numeric model (TELEMAC3D) to forecast energy results. A multi-criteria analysis was applied to the sustainability parameters.

2.1. Hydrodynamic Model

The TELEMAC system, developed by the Laboratoire National d'Hydraulique Environnement of the Company Electricité de France (CEDF), was used for the hydrodynamic simulations. The TELEMAC3D model solves the Navier-Stokes equations by considering local variations in the free surface of the fluid, neglecting density variations in the mass conservation equation and considering the hydrostatic pressure and Boussinesq approximations. The model is based on finite element techniques to solve the hydrodynamic equation [25] and relies on the sigma coordinate system to follow the surface and lower boundaries for vertical discretization [26].

A time step of 90 s and a Coriolis coefficient of $-7.70 \times 10^{-5} \text{ rad}\cdot\text{s}^{-1}$ (at 32°S) were used in all of the simulations. The horizontal turbulence process was performed using the Smagorinsky model. This closure turbulent model is generally used for maritime domains with large-scale eddy phenomena. It calculates the mixing coefficient by considering the size of the mesh elements and the velocity field [27].

The mixing length model for buoyant jets assessed the vertical turbulence processes and provided a better representation of the stratification. This model considers density effects via a damping factor that depends on the Richardson number to calculate the vertical diffusion coefficients.

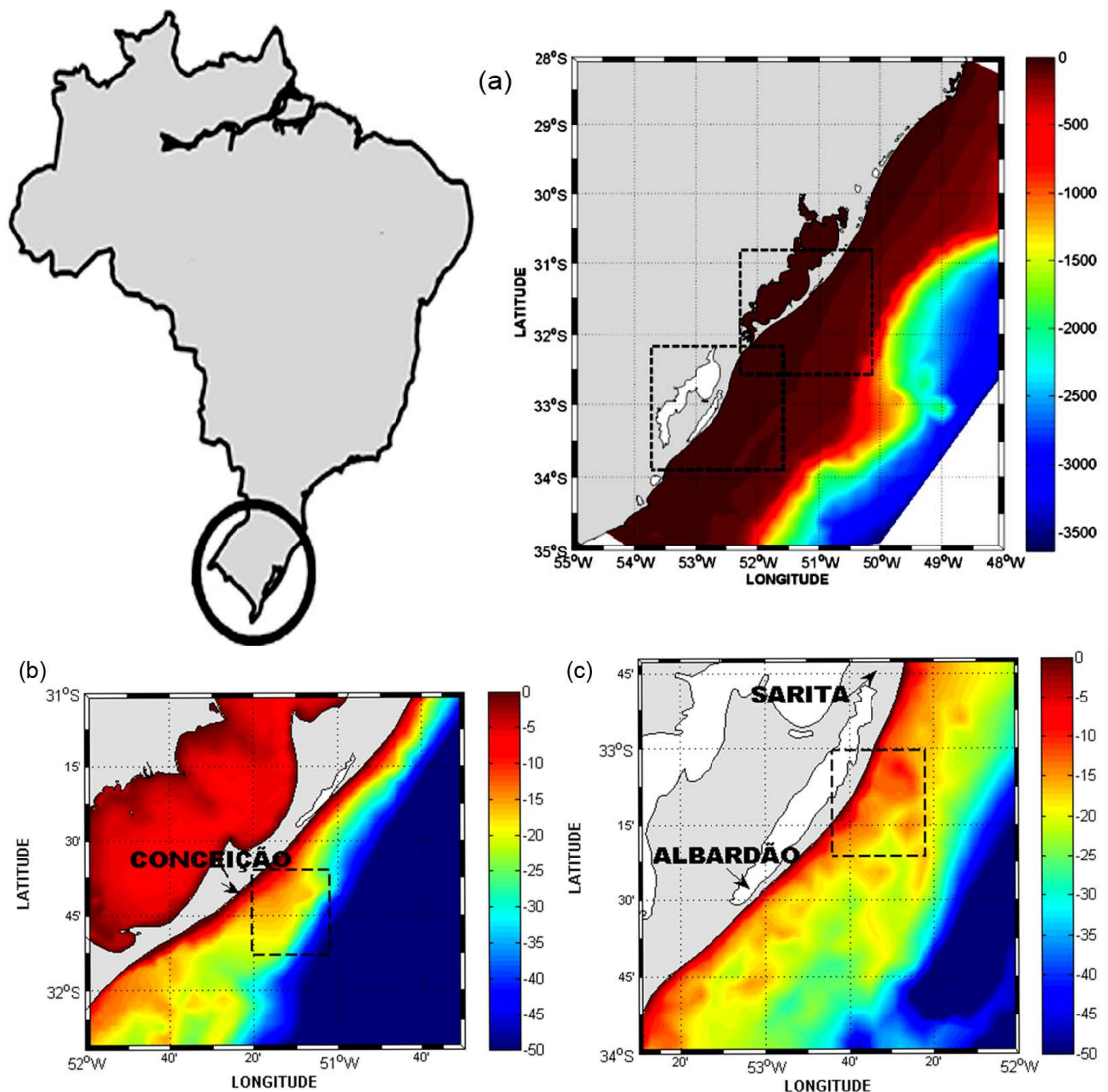


Figure 1. The study area. (a) The northern and southern study regions of the Southern Brazilian Shelf, with depths of approximately -3.500 m, are outlined with the dashed squares. (b) The northern region is depicted with the locations of the Solidão and Conceição lighthouses. (c) The southern region is located to the south of the Sarita lighthouse and to the north of the Albardão lighthouse.

2.2. Energy Conversion Module

The power of the ocean currents can be transformed using converters. Similar to the technology of wind converters, a submerged rotor is forced to rotate by the fluid surrounding it. A recent evaluation of the equipment available to capture hydrokinetic energy found that 76 pieces of equipment, including turbines, were in operation or were in the early stages of research [28].

The hydrodynamic simulations used in this study were produced using the TELEMAC3D model. The investigations involving energy conversion from the currents into electrical power were performed with the energy module [14]. This module uses the turbine standard equation (Equation (1)) to calculate the electric power in watts (W) from the incident flow velocity (where: ρ is the water density; η is the efficiency coefficient; A is the blade area and v is the incident velocity). **Table 1** indicates the turbine technical parameters used in the energy conversion module.

$$P(W) = \frac{1}{2} \eta \rho A v^3 \tag{1}$$

Table 1. Turbine technical parameters.

| Parameters | Value |
|------------------------|---------|
| Start-In Speed | 0.2 m/s |
| Cut-In Speed | 1.5 m/s |
| Efficiency Coefficient | 0.35 |
| Nominal Power | 170 kW |
| Turbine Height | 14 m |
| Turbine Ray | 10 m |

2.3. Initial and Boundary Conditions

The water body boundaries used in this study were the Guaíba River, the Camaquã a River and the São Gonçalo Channel (**Figure 2**) based on the discharge time series obtained from the Brazilian National Water Agency¹ (ANA) web-site. The discharge of the São Gonçalo Channel was assumed to be constant at 760 m³/s due to the absence of the observed data series [29].

The oceanic boundary was forced by the astronomical tides, water levels, current velocity, salinity and temperature fields. The salinity and temperature fields used as the initial conditions were obtained from the Ocean Circulation and Climate Advanced Modeling Project² (OCCAM).

The numerical model was initialized from the remaining parameters with a water level of 0.75 m, the approximate average tide in the region [30]. The amplitude and phase data on the oceanic border were calculated with the Grenoble Model FES95.2 (Finite Element Solution v. 95.6). The temporal and spatial variability of the winds and air temperature on the surface boundary were obtained from the National Oceanic and Atmospheric Administration (NOAA)³ website. The air temperature data on the ocean surface were also used to assess the heat exchange with the atmosphere in the model calculations.

The study was based on a two-year simulation (1998 and 1999). The first year represented anomalous conditions due to the ENSO influence, with moderate to high discharges occurring over the entire year. The second year represented normal conditions, when the freshwater discharge of the Patos Lagoon followed its natural pattern.

2.4. Calibration and Validation

Monteiro *et al.* [31]-[33] presented results for the calibration and validation of the two-dimensional model in the Patos Lagoon estuary. Subsequently, Marques *et al.* [14] [23] [24] [34] performed a set of simulations for the calibration and validation of the three-dimensional numerical model along the area covered by the Patos Lagoon and the adjacent coastal region.

The results of these calibration and validation tests indicated that the TELEMAC3D model can be used for studies of the SBS with an acceptable degree of accuracy. As a result, the values for many physical parameters (such as the wind influence coefficient, friction coefficient and turbulence models) were available and were used to conduct this study.

2.5. Analytical Hierarchy Process (AHP)

The AHP is widely used for multi-criteria analysis [6] [7] [35]-[38]. This analysis evaluated all of the criteria/factors which were considered relevant for decision, and compared against each other in a pair-wise comparison matrix. For the assemblage of this matrix, [39] and [40] suggested a scale for comparison that consisted of values ranging from 1 to 9 to describe the intensity of importance (preference/dominance).

The assigned preference values are synthesized to determine a ranking of the relevant factors in terms of a numerical value which is equivalent to the weights of the factors, where a value of 1 expressed equal importance

¹<http://www.ana.gov.br>

²<http://www.noc.soton.ac.uk/JRD/OCCAM/EMODS/>

³<http://www.cdc.noaa.gov/data/reanalysis/reanalysis.shtml>

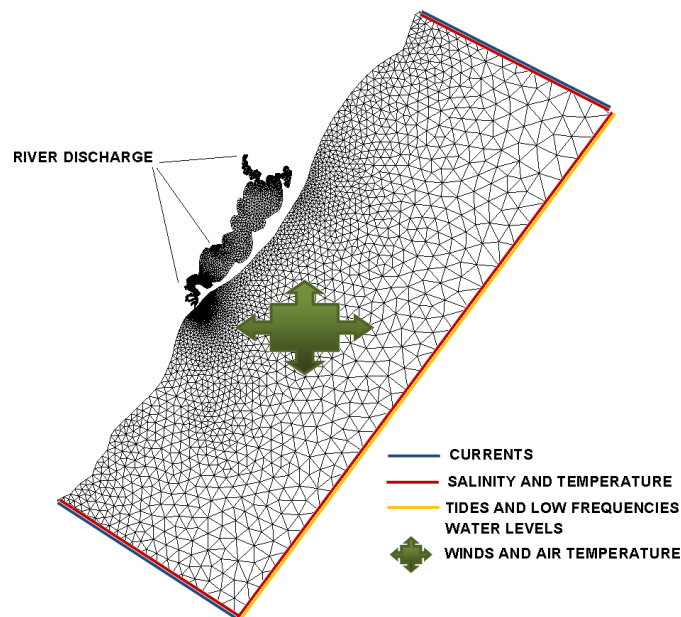


Figure 2. The finite elements mesh highlighting the liquid and surface boundaries conditions for the TELEMAC3D model.

and a value of 9 was given to those factors that had an extreme importance over another factor. Therefore the eigenvalues and eigenvectors of the square preference matrix are calculated, revealing important details about patterns in the data matrix.

After the preference matrix is performed, each pair-wise match receives a consistency index, which is directly calculated from the matrix with the Equation (2), where λ_{max} is the greatest eigenvalue of the preference matrix, while n is the order of the matrix.

$$CI = \frac{\lambda_{max} - n}{n - 1} \quad (2)$$

Therefore [39] provided the consistency ratio CR (Equation (3)) which is a single numerical index to check for consistency of the pair-wise comparison matrix. It is defined as the ratio of the consistency index (CI) to an average consistency index (RI), where RI depends on the order of the preference matrix [40]. Accordingly, a consistency ratio (CR) was provided after applying all of the criteria/factors in the comparison matrix. Saaty [40] recommended that the CR should never exceed a value of 0.1, otherwise the preference matrix should be reviewed.

$$CR = \frac{CI}{RI} \quad (3)$$

This methodology was applied using the Geographic Information System (GIS) Software, which is a tool for geoprocessing information with high liability. The criteria/factors were divided into 3 themes called: 1) Positive Factors; 2) Negative Factors; and 3) Restraining Factors. Each group was filled with information from Internet geodatabases, such as ANEEL⁴, IBGE⁵, MMA⁶, IBAMA⁷, DHN⁸, GISMAPS⁹ and results from the hydrodynamic simulation from TELEMAC3D.

This information and their scale values are shown in **Table 2**, where the subclasses (factors) were chosen according to several studies [6] [7] [35]-[38] [41]-[45]. According to Brazil's Policy, none installment may be per-

⁴<http://sigel.aneel.gov.br/brasil/viewer.htm>

⁵<ftp://geofp.ibge.gov.br/>

⁶<http://mapas.mma.gov.br/i3geo/>

⁷<http://siscom.ibama.gov.br/sitescr/>

⁸<http://www.dhn.mar.mil.br>

⁹<http://www.gismaps.com>

Table 2. Factors applied for the AHP analysis.

| Theme | Classes | Subclasses | Weight |
|----------------------------------|-----------------------------------------------------|-----------------------|--------|
| Positive | Energy production | | 0.3000 |
| | Bathymetric data | | 0.7000 |
| Negative | Transmission and Transport (n = 6) (CR = 0.0589) | Submarine Cables | 0.1267 |
| | | Substations | 0.2336 |
| | | Harbors | 0.3038 |
| | | Electric Transmission | 0.1333 |
| | | Roads | 0.0706 |
| | | Distance coast-sea | 0.1320 |
| | Sediment data (CR = 0.0446) | Silt | 0.0783 |
| | | Sand | 0.2484 |
| | | Gravel | 0.5263 |
| | | Clay | 0.1021 |
| Mud | | 0.0449 | |
| Geological data (CR = 0.0658) | Dredge Discharge zones | * | |
| | Paleontological sites | * | |
| | Archaeological sites | * | |
| Socioeconomic (CR = 0.0173) | Shores | 0.0650 | |
| | Economic Fishing zone | 0.1095 | |
| | Geo-parks | 0.0431 | |
| | Population | 0.2634 | |
| | Urban area | 0.5189 | |
| Restraining | Conservation Units | | * |
| | Endangered Species (CR = 0.0672) | Turtles | 0.2952 |
| | | Mammals | 0.1422 |
| | | Benthic | 0.3775 |
| | | Birds | 0.0524 |
| | | Elasmobranches | 0.0916 |
| | | Fish | 0.0411 |

*: Classes with an asterisk were used to create a mask to identify the study track.

formed in a Conservation Unit, paleontological or archaeological sites. In addition, dredge discharge zones were included as a non-suitable spot for the study due to the constant dredging activities in the Rio Grande Harbor, turning these zones inappropriate due to navigation and sediment release. These factors (shown in **Table 2** as an asterisk) were used as a mask in order to identify the forbidden places for the installment and also, the study track in which the factors were compared.

3. Results and Discussion

3.1. Energy Results

The possible installment locations of the turbines are highlighted in **Figure 1**. These locations are referred to in the following sections as the northern region (between the Solidão lighthouse and the Conceição Lighthouse) (**Figure 1(b)**) and the southern region (south of the Sarita lighthouse and north of the Albardão lighthouse)

(Figure 1(c)).

In these regions, the average velocity of the current (Figure 3(a)) was analyzed. The mean values that reached extremes of 0.4 m/s were found with high standard deviations of the current velocity and appeared in the same regions as the mean values (Figure 3(b)). This result suggested that these regions were suitable for power conversion. However, these regions can also go through periods of low power generation because the velocity deviation had a value closer to the average.

The isobaths were closer in the northern region (Figure 4(a)) and presented a stronger vertical gradient. In this region it was possible to find an average power (Figure 4(a)) of approximately 7 kW/day. The power conversion was intensified in the region where the isobaths were farther apart (the 20 m isobath). The average power in this region reached 10 kW/day.

This area was characterized by complex topography, with the 50 m isobaths (the limit of the inner shelf) closer to the shoreline, where there was a high gradient. The gradient was reduced towards the Conceição Lighthouse, where this isobath moves away from the shore. Thus, the circulation pattern was modified when a current flowed from the region (with the 50 m isobaths near the coast) to where the coastal flow was more intense and concentrated in a shallower region near the 20 m isobath. The flow slowed down and spread out as this process occurred. Intensification occurred in the northern region when the current at the 20 m isobath encountered a topographic strangulation, diverting the current to the 30 m isobath and increasing its velocity.

The southern region (Figure 4(b)) had a distinct pattern of bathymetry in which the isobaths were far apart. However, the submarine floor had major irregularities. The high values of the average power were observed over almost the entire length of the inner shelf, between 10 and 20 m deep. Average power values (Figure 4(b)) near 3.5 kW/day were observed in this region.

The southern region had a complex bathymetry with significant linear banks, such as the Bank of Albardão, and a large depression (the Albardão Pit at a 75 m depth). The Bank of Albardão acts as a barrier to the coastal current (directed by the 20 m isobaths) causing the flow to diverge. Consequently, the meandering of the current intensified, suggesting that the intensification of power in this region was strongly influenced by the irregular topography.

This region relies on its oceanographic features, while the northern region was highly dominated by a strong vertical gradient which generated squeezing and stretching currents, enhancing the power generation. The southern region was forced by a topographic feature (e.g., the Bank of Albardão) that forced the flow to diverge, and, as a consequence, the meandering of the current intensified, increasing the power availability in this region.

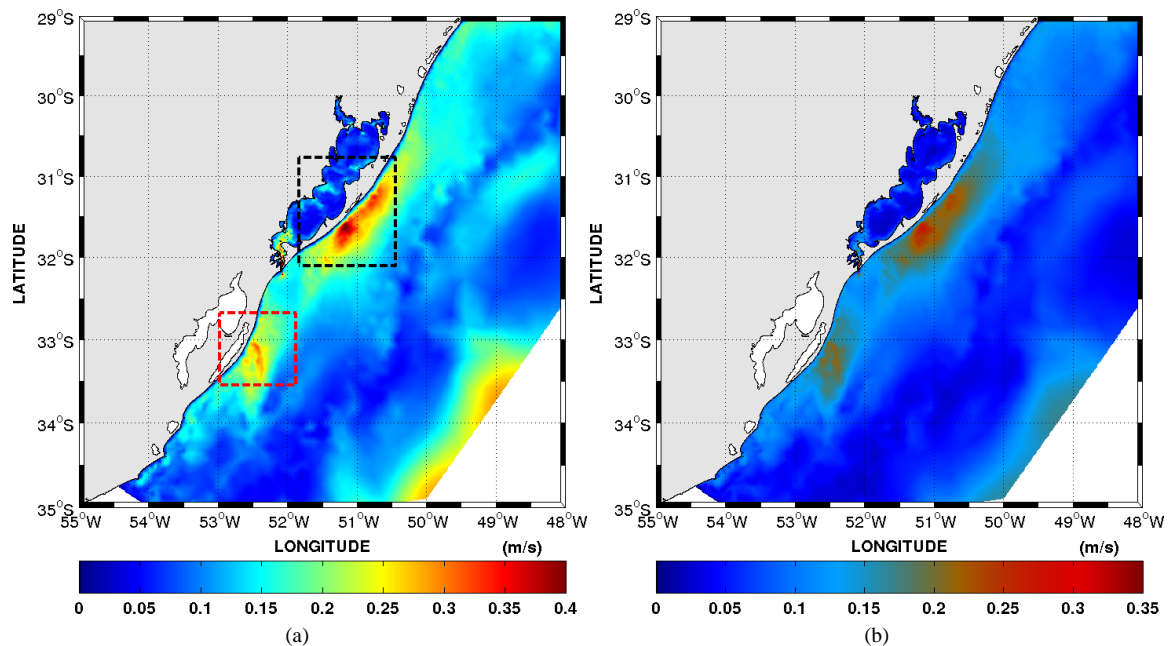


Figure 3. (a) Average current velocity (m/s) and its standard deviation (b) during the entire simulation period. In detail, the southern region in the red-dashed area, and the northern region on the black-dashed area.

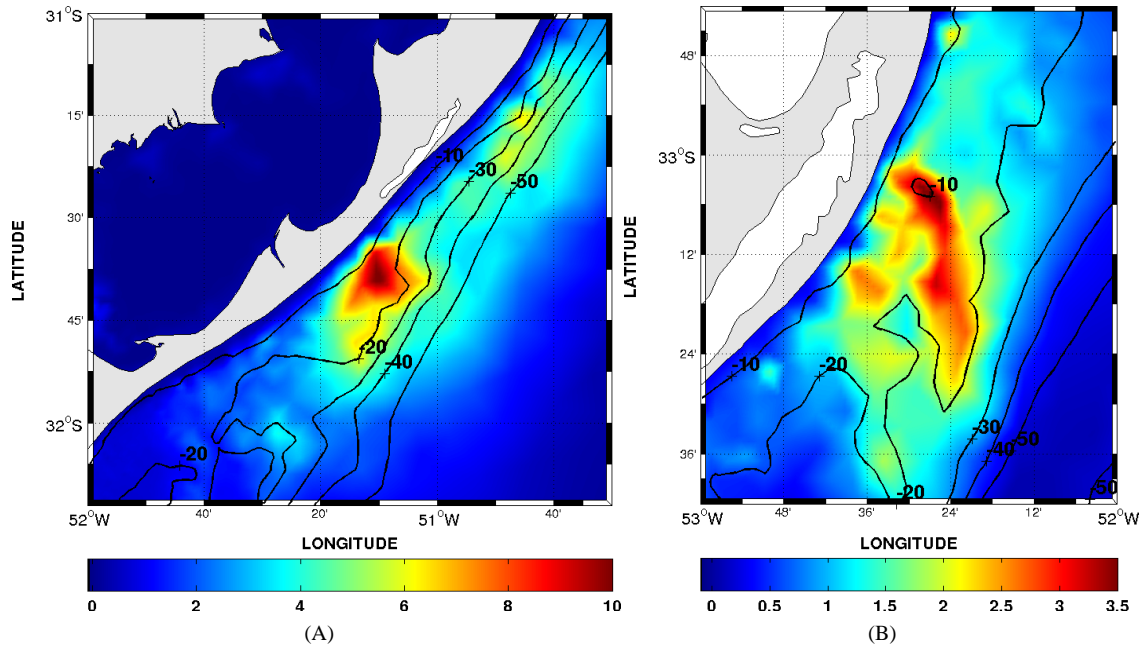


Figure 4. Analysis of the mean power (kW/day). (a) Northern region; (b) Southern region. The isolines range from 0 m to -50 m.

3.2. Identification of Installation Sites

The suitable installation areas were determined by the level of power density, the ease of accessibility and the number of environmental conflicts with the site selection methodology. Although the weight of each factor depends on the interference of the stakeholder, the AHP method relies on a very advanced consistency method to avoid misleading decisions.

The AHP was applied on each subclass and gathered them as a new class (their Consistency Ratio is shown on [Table 2](#)). Classes were intersected and reduced from the restraining factors to concatenate all of the information on a final map. The restraining factors consisted of: 1) desirable bathymetry for installation (0 to -50 m); 2) Endangered Species; and 3) Proximity to Conservation Units.

The positive factors were formed by gathering the energy information from the hydrodynamic model and the bathymetric data (especially the data above 50 m, see [Figure 5\(a\)](#)). The negative factors were formed by a convolution of the data that resulted from the three major shapes ([Figures 5\(b\)-\(d\)](#)) of the transmission and transport data, the socioeconomic influence data and the geological data.

The relative importance of location factors is also changing as the decision process stages proceed [46]. In the early stage of identifying preferred geographical areas, only a few priority items are considered to identify those regions that satisfy most important criteria, such as the availability of strong currents or the proper bathymetry according to the turbine settings.

When reaching the stage of selecting specific locations, site-specific factors such as grain size, endangered species or access to roads and power cables may dominate over another location. In the final stage of evaluating a few selected factors may escalate in favor of another factor, or even, decrease the importance of other factors.

All of the shapes showed the study track of this work, which meant that the suitable area had to be inside of these lines. This mask was made by applying all of the restraining factors, as the incidence of endangered species and Conservation Units inhibited the possibility of using any area. It is feasible to compare the possible and less possible areas according to the blue and red colors in the charts, respectively. The transmission and transport shape ([Figure 5\(b\)](#)) was dominated by the presence of the Rio Grande Harbor (30%), due to its navigation importance, followed by the electric transmission and substation (23%) that were necessary to reduce the cost of installation in a desirable site.

The sediment data ([Figure 5\(c\)](#)) showed a few possible areas and there was a dominance of medium possible areas. This slight divergence is the result of the influence of the gravel, which received a high weight (52%) due

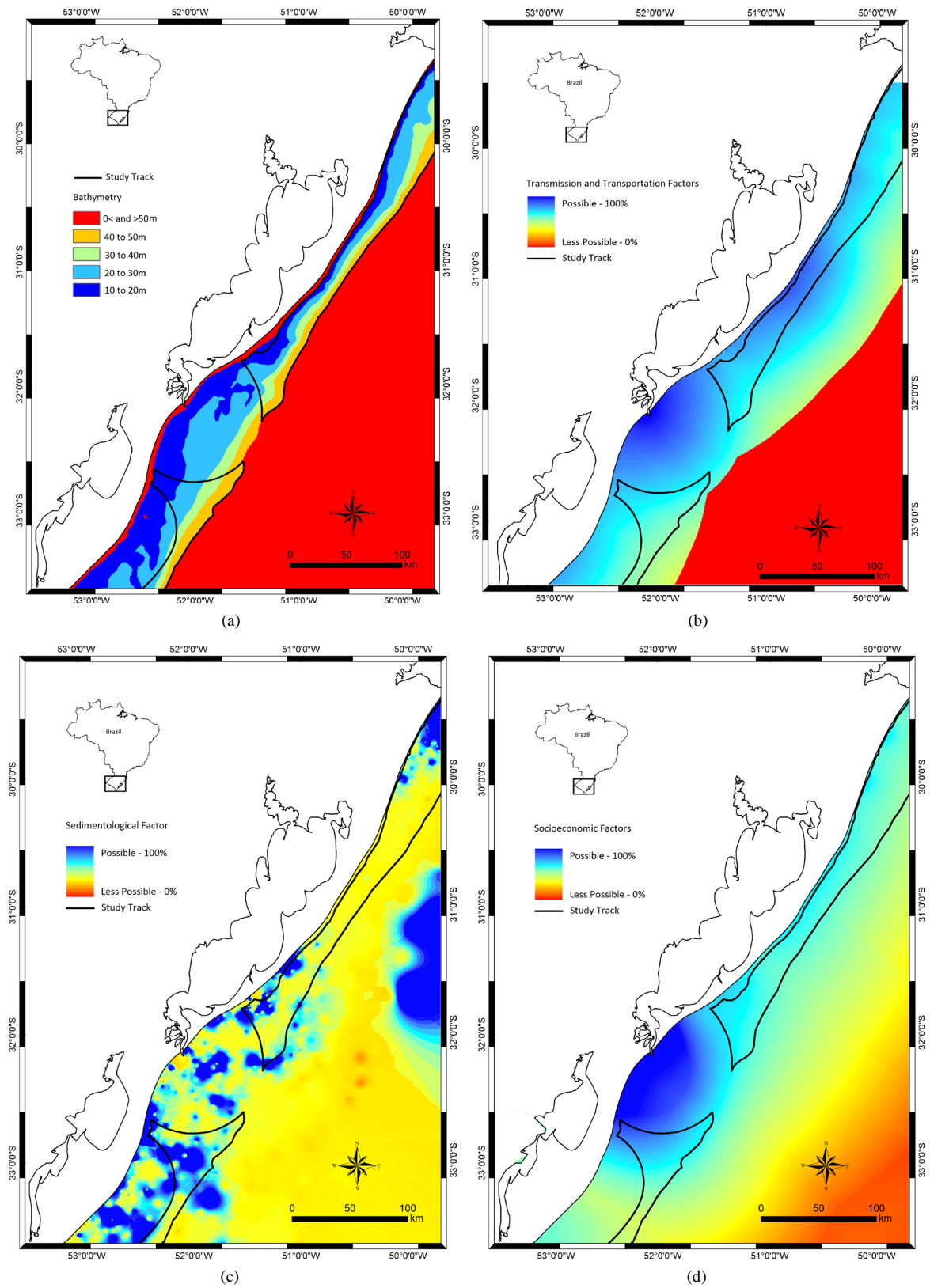


Figure 5. The AHP results: (a) bathymetric data; (b) transmission and transport; (c) sediment database; and (d) socioeconomic shape.

to its importance for the installation process. The sand had a weight of 24%. The socioeconomic shape (Figure 5(d)) was greatly influenced by the urban areas (such as Rio Grande City at 45%), and the population concentration was the second most important factor at 30%.

We achieved the shapes of the positive and negative factors by integrating the prior results on themes. The positive factors (Figure 6(a)) were strongly dominated by the energy production (Figure 4(a) and Figure 4(b)) and had a greater mean energy. This area was likely the best area for installation. The southern region had a 60% acceptance, but due to the presence of geological sites and Conservation Units, this region was cut from the study track. The northern region had less influence from constraining factors than the southern region, and its energy peak was located inside the study track.

The negative factors (Figure 6(b)) shape showed that the area near the Rio Grande jets was the least possible installation area, due to the importance of navigation in this area. The northern region had less possible installation areas than the surroundings of the southern region. This negative influence was justified by the proximity of the northern region to fishing zones and Conservation Units.

A final AHP was created by using all of the shapes. Figure 7 represents the mixing between negative and positive factors, which resulted in a shape dominated by less possibility, the white zone inside the study track represents areas with less than 1% of installment possibility. A minor region inside the most energetic area in the northern region was the most viable region. This result was highly dominated by the positive factors, such as energy production, which counter balanced all of the negative influences from nearby locations.

4. Conclusions

In the SBS, two regions were suitable for the installation of current energy converters. The northern region had the highest potential power, where a single converter could generate an average of 10 kW/day and could reach an integrated power conversion of 3.5 MW/year. The southern region had less potential power, generating an average of 3.5 kW/day and integrated values of 1.5 MW/year. Both regions had intense oceanographic features that dominated the current velocities.

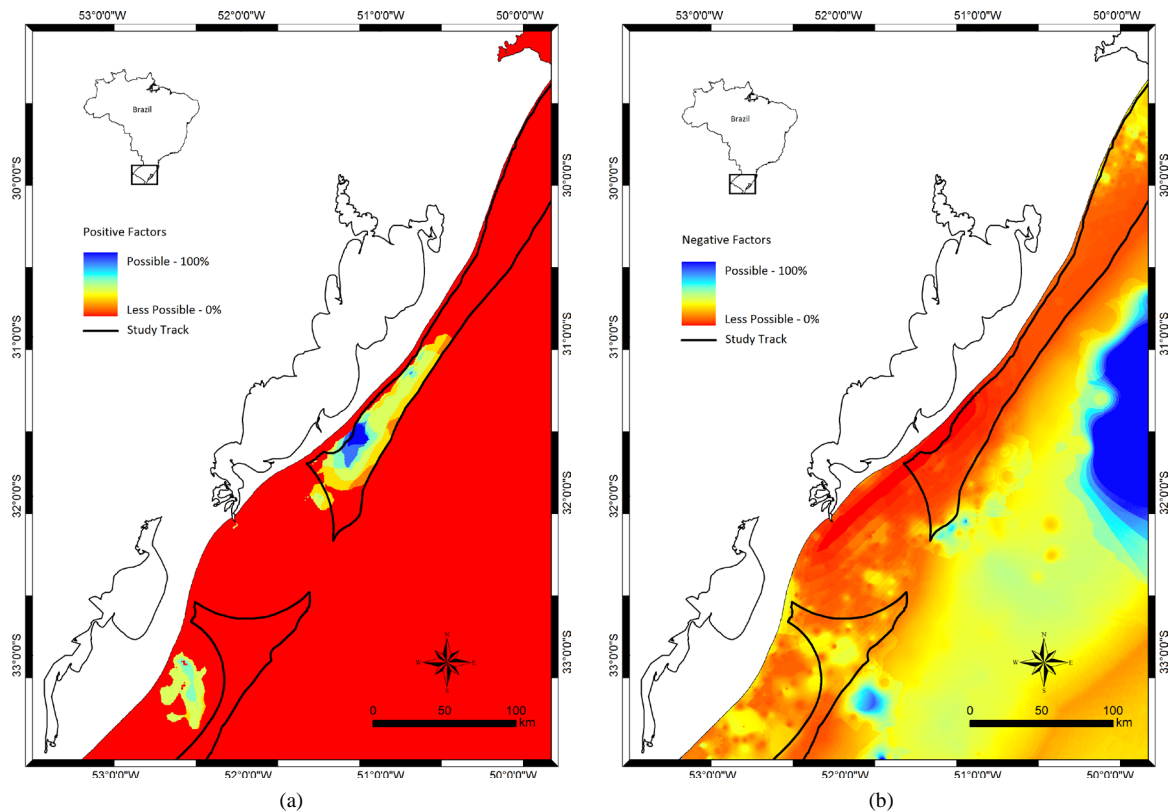


Figure 6. The AHP results: (a) positive factors and (b) negative factors.

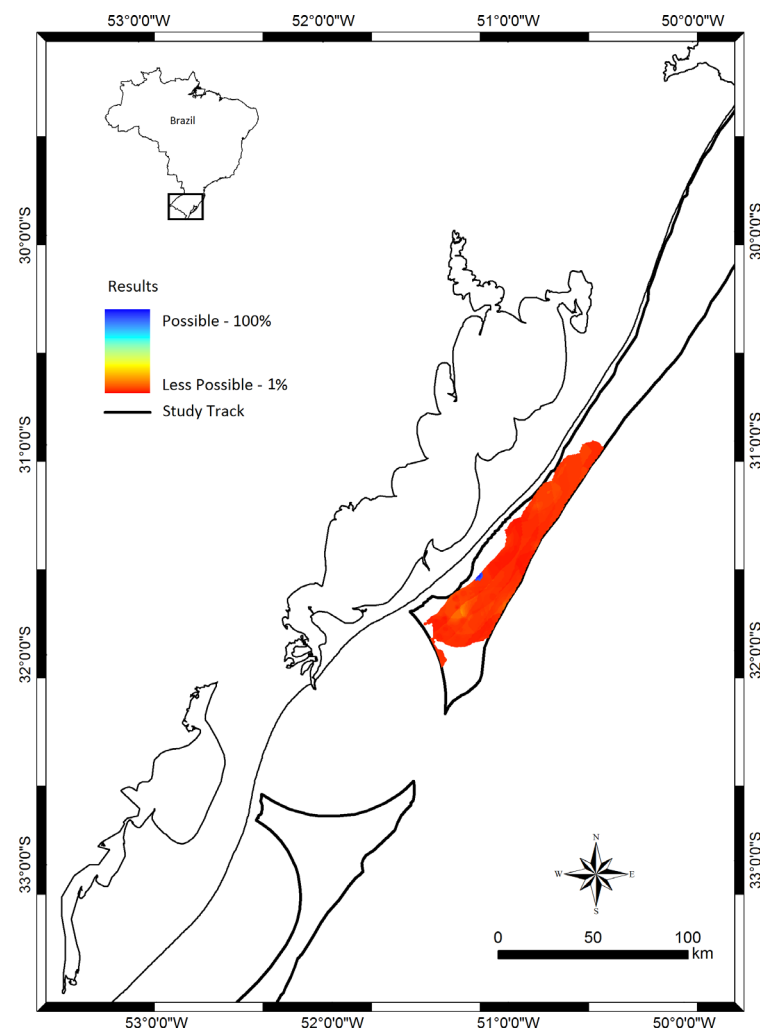


Figure 7. Most viable areas for installation.

The suitable sites for tidal power conversion were marked and evaluated based on three major themes: Negative factors; positive factors; and restraining factors. The TELEMAC3D results were evaluated against all of the socioeconomic, geological and environmental results available. The study aimed for an environmentally friendly result between these variables.

The study showed that the depth constraints, human activities in the coastal zone and the sensitive biological resources limited the amount of suitable locations for a marine current turbine facility. Due to the relatively strong energy conversion in the northern region, this area emerged as a possible place for a turbine. The AHP proved to be a powerful asset for selecting suitable locations.

Despite the results found in this work, the AHP can serve as a useful preliminary analysis tool for decision makers before allocating resources for a more detailed evaluation. Further studies should apply more data into the analysis to achieve more precise results.

Acknowledgements

The authors are grateful to the Agência Nacional do Petróleo-ANP and Petrobras for the fellowships regarding the Programa de Recursos Humanos (PRH-27) that provided bursaries, the Fundação de Amparo à Pesquisa do Estado do Rio Grande do Sul (FAPERGS) for sponsoring this research under contract: 1799123 and to the Conselho Nacional de Desenvolvimento Científico e Tecnológico (CNPq) under contracts: 456292/2013-6 and 305885/2013-8. Further acknowledgments go to the Brazilian Navy for providing detailed bathymetric data for

the coastal area; the Brazilian National Water Agency and NOAA for supplying the fluvial discharge and wind data sets, respectively; and to the open TELEMAC-MASCARET (www.opentelemac.org) for providing the academic license of the TELEMAC system to accomplish this research. Although some data were taken from governmental databases, this paper is not necessarily representative of the views of the government.

References

- [1] Brundtland, G.H. (1987) *Our Common Future*. Oxford University Press, Oxford.
- [2] Elkington, J. (1994) Towards the Sustainable Corporation: Win-Win-Win Business Strategies for Sustainable Development. *California Management Review*, **36**, 90. <http://dx.doi.org/10.2307/41165746>
- [3] IPCC (2001) *Climate Change 2001: The Scientific Basis in the Climate System, an Overview*.
- [4] Swisher, J.N., Jannuzz, G.S.D.M. and Redlinger, R.Y. (1997) Tools and Methods for Integrated Resource Planning: Improving Energy Efficiency and Protecting the Environment.
- [5] Wang, J.J., Jing, Y.Y., Zhang, C.F. and Zhao, J.H. (2009) Review on Multi-Criteria Decision Analysis Aid in Sustainable Energy Decision-Making. *Renewable and Sustainable Energy Reviews*, **19**, 2263-2278. <http://dx.doi.org/10.1016/j.rser.2009.06.021>
- [6] Cowan, K., Daim, T. and Anderson, T. (2010) Exploring the Impact of Technology Development and Adoption for Sustainable Hydroelectric Power and Storage Technologies in the Pacific Northwest United States. *Energy*, **35**, 4771-4779. <http://dx.doi.org/10.1016/j.energy.2010.09.013>
- [7] Defne, Z., Haas, K.A. and Fritz, H.M. (2011) GIS Based Multi-Criteria Assessment of Tidal Stream Power Potential: A Case Study. *Renewable and Sustainable Energy Reviews*, **15**, 2310-2321. <http://dx.doi.org/10.1016/j.rser.2011.02.005>
- [8] Defne, Z., Haas, K.A., Fritz, H.M., Jiang, L., French, S.P., Shi, X., Smith, B.T., Neary, V.S. and Stewart, K.M. (2012) National Geodatabase of Tidal Stream Power Resource in USA. *Renewable and Sustainable Energy Reviews*, **16**, 3326-3338. <http://dx.doi.org/10.1016/j.rser.2012.02.061>
- [9] Feizizadeh, B. and Haslauer, E.M. (2012) GIS-Based Procedures of Hydropower Potential for Tabriz Basin, Iran. *International Journal*, 495-502.
- [10] Yue, C.-D. and Yang, G.G.-L. (2007) Decision Support System for Exploiting Local Renewable Energy Sources: A Case Study of the Chigu Area of Southwestern Taiwan. *Energy Policy*, **35**, 383-394. <http://dx.doi.org/10.1016/j.enpol.2005.11.035>
- [11] Yue, C.-D. and Wang, S.-S. (2006) GIS-Based Evaluation of Multifarious Local Renewable Energy Sources: A Case Study of the Chigu Area of Southwestern Taiwan. *Energy Policy*, **34**, 730-742. <http://dx.doi.org/10.1016/j.enpol.2004.07.003>
- [12] Capeletto, G.J. and De Moura, G.H.Z. (2010) Balanço Energético do Rio Grande do Sul 2010: Ano base 2009.
- [13] Kirinus, E.P., Marques, W.C. and Stringari, C.E. (2012) Viabilidade de conversão da energia de correntes marinhas na Plataforma Continental Sul do Brasil. *Vetor*, **22**, 83-103.
- [14] Marques, W.C., Fernandes, E.H.L., Malcherek, A. and Rocha, L.A.O. (2011) Energy Converting Structures in the Southern Brazilian Shelf: Energy Conversion and Its Influence on the Hydrodynamic and Morphodynamic Processes. *Journal of Earth Sciences and Geotechnical Engineering*, **1**, 61-85.
- [15] Zembruski, S. (1979) Geomorfologia da margem continental sul brasileira e das bacias oceânicas adjacentes. In: Chaves, H.A.F., Ed., *Geomorfologia da margem continental Brasileira e das áreas oceânicas adjacentes*, Projeto REMAC n° 7, Rio de Janeiro, 129-174.
- [16] Castro, B.M., Lorenzetti, J.A., Silveira, I.C.A. and Miranda, L.B. (2006) Chapter 1: Estrutura termohalina e circulação na região entre o Cabo de São Tomé (RJ) e o Chuí (RS). In: Rossi-Wongtschowski, C.L.D.B., Ed., *O ambiente oceanográfico da plataforma continental e do talude na região sudeste-sul do Brasil*, Edusp, São Paulo, 11-20.
- [17] Möller, O.O.J., Piola, A.R., Freitas, A.C. and Campos, E.J.D. (2008) The Effects of River Discharge and Seasonal Winds on the Shelf off Southeastern South America. *Continental Shelf Research*, **28**, 1607-1624. <http://dx.doi.org/10.1016/j.csr.2008.03.012>
- [18] Chelton, D.B., Schlax, M.G., Witter, D.L. and Richmann, J.G. (1990) GEOSAT Altimeter Observations of the Surface Circulation of the Southern Ocean. *Journal of Geophysical Research*, **95**, 877-903. <http://dx.doi.org/10.1029/JC095iC10p17877>
- [19] Piola, A.R. and Matano, R.P. (2001) The South Atlantic Western Boundary Currents Brazil/Falkland (Malvinas) Currents. In: Steele, J.M., Thorpe, S.A. and Turekian, K.K. Eds., *Encyclopedia of Ocean Sciences*, Academic Press, Walham, MA, 340-349.
- [20] Gordon, A.L. (1989) Brazil-Malvinas Confluence—1984. *Deep-Sea Research*, **36**, 359-384.

- [http://dx.doi.org/10.1016/0198-0149\(89\)90042-3](http://dx.doi.org/10.1016/0198-0149(89)90042-3)
- [21] Piola, A.R., Matano, R.P., Palma, E.D., Möller, O.O. and Campos, E.J.D. (2005) The Influence of the Plata River Discharge on the Western South Atlantic Shelf. *Geophysical Research Letters*, **32**, Article ID: L01603.
- [22] Braga, M.F. and Krusche, N. (2000) Padrão de ventos em Rio Grande, RS, no período de 1992 a 1995. *Atlântica*, **22**, 27-40.
- [23] Marques, W.C., Fernandes, E.H.L., Monteiro, I.O. and Möller, O.O. (2009) Numerical Modeling of the Patos Lagoon Coastal Plume, Brazil. *Continental Shelf Research*, **29**, 556-571. <http://dx.doi.org/10.1016/j.csr.2008.09.022>
- [24] Marques, W.C., Fernandes, E.H.L. and Moller, O.O. (2010) Straining and Advection Contributions to the Mixing Process of the Patos Lagoon Coastal Plume, Brazil. *Journal of Geophysical Research*, **115**, Article ID: C06019. <http://dx.doi.org/10.1029/2009JC005653>
- [25] Hervouet, J.M. (2007) *Hydrodynamics of Free Surface Flows: Modelling with the Finite Element Method*. John Wiley & Sons, Hoboken.
- [26] Hervouet, J.M. and Van Haren, L. (1996) Recent Advances in Numerical Methods for Fluid Flows. In: Anderson, M.G., Walling, D.E. and Bates, P.D., Eds., *Floodplain Processes*, Wiley, New York, 183-214.
- [27] Smagorinsky, J. (1963) General Circulation Experiments with the Primitive Equation, I. The Basic Experiment. *Weather Review*, **91**, 99-164. [http://dx.doi.org/10.1175/1520-0493\(1963\)091<0099:GCEWTP>2.3.CO;2](http://dx.doi.org/10.1175/1520-0493(1963)091<0099:GCEWTP>2.3.CO;2)
- [28] Khan, M.J., Bhuyan, G., Iqbal, M.T. and Quaicoe, J.E. (2009) Hydrokinetic Energy Conversion Systems and Assessment of Horizontal and Vertical Axis Turbines for River and Tidal Applications: A Technology Status Review. *Applied Energy*, **86**, 1823-1835. <http://dx.doi.org/10.1016/j.apenergy.2009.02.017>
- [29] Viegas, J.S. and Franz, A.F.H. (2006) Hidrologia do Canal de São Gonçalo. Tech. Rep., FURG-UFPEL, Pelotas.
- [30] Möller, O.O., Castaing, P., Salomon, J.C. and Lazure, P. (2001) The Influence of Local and Non-Local Forcing Effects on the Subtidal Circulation of Patos Lagoon. *Estuaries*, **24**, 297-311. <http://dx.doi.org/10.2307/1352953>
- [31] Monteiro, I.O., Pearsom, M., Möller, O.O. and Fernandes, E.H.L. (2006) Hidrodinâmica do Saco da Mangueira: Mecanismos que controlam as trocas com o estuário da Lagoa dos Patos. *Atlântica*, **27**, 8-101.
- [32] Fernandes, E.H.L., Monteiro, I.O. and Möller, O.O. (2007) On the Dynamics of Mangueira Bay—Patos Lagoon (Brazil). *Journal of Coastal Research*, **10047**, 97-107. <http://dx.doi.org/10.2112/1551-5036-47.sp1.97>
- [33] Fernandes, E.H.L., Dyer, K.R., Möller Jr., O.O. and Niencheski, L.F. (2002) The Patos Lagoon Hydrodynamics during an El Niño Event (1998). *Continental Shelf Research*, **22**, 1699-1713. [http://dx.doi.org/10.1016/S0278-4343\(02\)00033-X](http://dx.doi.org/10.1016/S0278-4343(02)00033-X)
- [34] Marques, W.C., Fernandes, E.H., Möller Jr., O.O., Moraes, B.C. and Malcherek, A. (2010) Dynamics of the Patos Lagoon Coastal Plume and Its Contribution to the Deposition Pattern of the Southern Brazilian Inner Shelf. *Journal of Geophysical Research*, **115**, Article ID: C10045. <http://dx.doi.org/10.1029/2010JC006190>
- [35] Eldrandaly, K., Eldin, N. and Sui, D. (2003) A COM-Based Spatial Decision Support System for Industrial Site Selection. *Journal of Geographic Information and Decision Analysis*, **7**, 72-92.
- [36] Karnatak, H.C., Saran, S., Bhatia, K. and Roy, P.S. (2007) Multicriteria Spatial Decision Analysis in Web GIS Environment. *GeoInformatica*, **11**, 407-429. <http://dx.doi.org/10.1007/s10707-006-0014-8>
- [37] Seabra, V.S., da Silva, G.C. and Cruz, C.B.M. (2008) The Use of Geoprocessing to Assess Vulnerability on the East Coast Aquifers of Rio de Janeiro State, Brazil. *Environmental Geology*, **57**, 665-674. <http://dx.doi.org/10.1007/s00254-008-1345-6>
- [38] Sabri, S., Majid, M.R. and Ludin, A.N.M. (2010) Modeling Smart Growth Components in an Integrated Multicriteria-GIS Environment. *Proceedings of the 3rd International Graduate Conference on Engineering, Science, and Humanities*, Johor, 2-4 November 2010, 1-6.
- [39] Saaty, T.L. (1977) A Scaling Method for Priorities in Hierarchical Structures. *Journal of Mathematical Psychology*, **15**, 231-281. [http://dx.doi.org/10.1016/0022-2496\(77\)90033-5](http://dx.doi.org/10.1016/0022-2496(77)90033-5)
- [40] Saaty, T.L. and Vargas, L.G. (1991) *Prediction, Projection and Forecasting*. Kluwer Academic Publishers, Norwell, 251. <http://dx.doi.org/10.1007/978-94-015-7952-0>
- [41] Voivontas, D., Assimacopoulos, D., Mourelatos, A. and Corominas, J. (1998) Evaluation of Renewable Energy Potential Using a GIS Decision Support System. *Renewable Energy*, **13**, 333-344. [http://dx.doi.org/10.1016/S0960-1481\(98\)00006-8](http://dx.doi.org/10.1016/S0960-1481(98)00006-8)
- [42] Prest, R., Daniell, T. and Ostendorf, B. (2007) Using GIS to Evaluate the Impact of Exclusion Zones on the Connection Cost of Wave Energy to the Electricity Grid. *Energy Policy*, **35**, 4516-4528. <http://dx.doi.org/10.1016/j.enpol.2007.02.033>
- [43] Nobre, A., Pacheco, M., Jorge, R., Lopes, M. and Gato, L. (2009) Geo-Spatial Multi-Criteria Analysis for Wave Ener-

- gy Conversion System Deployment. *Renewable Energy*, **34**, 97-111. <http://dx.doi.org/10.1016/j.renene.2008.03.002>
- [44] Yang, J. and Lee, H. (1997) An AHP Decision Model for Facility Location Selection. *Facilities*, **15**, 241-254. <http://dx.doi.org/10.1108/02632779710178785>
- [45] Tavares, G., Zsigraiová, Z. and Semiao, V. (2011) Multi-Criteria GIS-Based Siting of an Incineration Plant for Municipal Solid Waste. *Waste Management*, **31**, 1960-1972. <http://dx.doi.org/10.1016/j.wasman.2011.04.013>
- [46] Haigh, R. (1990) Selecting a US Plant Location: The Management Decision Process in Foreign Companies. *Columbia Journal of World Business*, 22-31.

Scientific Research Publishing (SCIRP) is one of the largest Open Access journal publishers. It is currently publishing more than 200 open access, online, peer-reviewed journals covering a wide range of academic disciplines. SCIRP serves the worldwide academic communities and contributes to the progress and application of science with its publication.

Other selected journals from SCIRP are listed as below. Submit your manuscript to us via either submit@scirp.org or [Online Submission Portal](#).

